Scanning Microscopy

Volume 10 | Number 1 Article 10

1-16-1996

A Novel Method for Viewing Heavy Metal Stained and Embedded Biological Tissue by Field Emission Scanning Electron Microscopy

R. Geoffrey Richards
AO/ASIF Research Institute, richards@ccgate.ari.ch

Iolo ap Gwynn
The University of Wales

Scanning Microscopy, Vol. 10, No. 1, 1996 (Pages 111-119) 0891-7035/96$5.00+.25
Scanning Microscopy International, Chicago (AMF O'Hare), IL 60666 USA

A NOVEL METHOD FOR VIEWING HEAVY METAL STAINED AND EMBEDDED BIOLOGICAL TISSUE BY FIELD EMISSION SCANNING ELECTRON MICROSCOPY

R. Geoffrey Richards* and Iolo ap Gwynn[1]

AO/ASIF Research Institute, Clavadeler Strasse, CH-7270 Davos, Switzerland
[1]Institute of Biological Sciences, The University of Wales, Aberystwyth, Wales, SY23 3DA, U.K.

(Received for publication July 26, 1995 and in revised form January 16, 1996)

Abstract

Backscattered electron (BSE) imaging was used to display heavy metal stained biological structures of various embedded specimens. Samples were fixed, stained and embedded in resin blocks as with preparation for the transmission electron microscope (TEM). Blocks were trimmed to center the specimens in a trapezoidal face of up to 5 mm^2 and their sides painted with conductive silver paint leaving the face uncovered. Blocks were sputter coated with 6-8 nm of silver, chromium or aluminum, with aluminum providing the best specimen contrast in BSE mode. Samples were examined in a field emission scanning electron microscope operated at a high emission current of 50 μA. Both the fixation protocol and microscope operating parameters were optimized to maximize the number of BSE available from the smallest probe. An accelerating voltage of 10 keV was found optimal for resolution and contrast. The technique allowed the direct visualization of embedded samples at resolutions beyond light microscopy with good contrast, without cutting sections, and avoiding grid bars obscuring areas of interest. The two dimensional images provided averaged information on the internal structures of the specimens in relation to the predicted emission depth of the BSE. The technique could be used for rapid diagnostics in pathological examinations, or for routine preselection of areas of interest within a sample face before final trimming for ultrathin sectioning for higher resolution TEM study.

Key Words: Field emission, scanning electron microscopy, backscattered electron imaging, atomic number contrast, pathology.

*Address for correspondence:
R.G. Richards
AO/ASIF Research Institute, ClavadelerStrasse,
CH-7270, Davos, Switzerland
Telephone number: (41) 81 414 23 97 (47)
FAX number: (41) 81 414 22 88
E.mail: richards@ccgate.ari.ch

Introduction

Backscattered electron (BSE) imaging with the scanning electron microscope (SEM) can be used to examine semi-thin sections of fixed and embedded tissues at medium resolution (Kushida *et al.*, 1982; Scala *et al.*, 1985; Nanci *et al.*, 1990). The SEM has also been used in secondary electron imaging mode to view sections of embedded specimens after removal of polymerized resin with a solvent (Wing-Ling *et al.*, 1982; Scala *et al.*, 1990, 1991), allowing TEM and SEM of the same sample.

The source depth of the BSE depends upon both the energy of the primary electron beam and the density of the sample. The maximum depth from which the BSE emerged at gun accelerating voltages of 3, 6 and 25 keV, as used by Kushida *et al.* (1982) in their BSE imaging of semi-thin sections, was between 0.08 mm and 2.7 mm. This can be calculated using the following expression as published by Kanaya and Okayama (1972),

$$R = 0.0276A\,E_0^{1.67} / Z^{0.89}\rho \ \text{(mm)} \qquad (1)$$

where R is the approximate depth of an "average" electron penetration into the specimen, E_0 is the primary beam energy (keV), A is the atomic weight in g/mol, Z is the atomic number and ρ is the density in g/cm^3. BSE are estimated to come from a maximum depth of approximately 0.2R (D.C. Joy, Personal communication, 1994). Though Kushida *et al.* (1982) used methacrylates, the properties of (London Resin) LR White acrylic resin should be similar (mean ρ = 0.98 g/cm^3, weighted average of A = 11.171 g/mol and weighted average of Z = 6.141 for the LR White formula). Therefore at 3, 6 and 25 keV the approximate depth of an "average" electron penetration (R) would be 0.4 mm, 1.25 mm and 13.5 mm respectively and the depth from which the BSE emerge would therefore be approximately 0.08 mm, 0.25 mm and 2.7 mm, respectively. This shows that with the thinner sections they used (0.3-0.5 mm), where they experienced poor contrast and image quality, this was due to the majority of the primary beam electrons

passing straight through the sections, and therefore, producing only a very low number of BSE from them. Although some of the primary beam electrons would also have penetrated the 1 mm sections, these sections gave good images at 6 keV where the maximum depth from which the BSE would have emerged was within the limits of the 1 mm section thickness, i.e., about 0.25 mm.

Optimization of the field emission electron microscope (FESEM) in BSE detection mode is made possible by using high emission currents. This increases the number of primary electrons interacting with the specimen, resulting in a higher number of BSE at any given accelerating voltage. This increase in BSE production has been used to produce a more beneficial signal-to-noise ratio. BSE imaging in such a mode has already been reported for fixed, stained and embedded cells at varying accelerating voltages, including low beam potentials (Richards and ap Gwynn, 1995).

In the work presented here, resin embedded biological specimens, differentially contrasted with heavy metal stains, are observed in the FESEM in BSE mode. Medium resolution is obtained by optimizing the microscope settings for a minimum spot size and a high emission current; this avoids the necessity of producing semi-thin sections for specimen evaluation. It also allows direct study of biological material with the FESEM, without the limiting factors associated with section surface area and thickness of specimens that can be introduced into the TEM. An added benefit is that grid bars cannot obscure areas of interest. The same material can be examined with the FESEM and, if required, subsequently sectioned and examined at high resolution with the TEM.

The reader is referred to Goldstein *et al.* (1992) for a general reference on electron specimen interactions and to Richards and ap Gwynn (1995) for text on BSE.

Material and Methods

Fixation

Various 1-3 mm^3 samples of biological tissue were examined: mouse intestinal villi, striated muscle, kidney, testis, liver and pancreas, cultured primary osteoblasts cells from rat juvenile calvaria and cercaria of *Parochis* parasites. All fixations were based around the addition of high contrast staining to the material with osmium tetroxide and uranyl acetate in exactly the same way as is done for TEM specimen preparation. A typical fixation was, as for the mouse tissue:

The samples were rinsed for 5 minutes in 0.1 M PIPES (Piperazine-NN'-bis-2-ethane sulphonic acid) (Fluka, Buchs, Switzerland) buffer, pH 7.4 at 293K. Primary fixation was in 2.5% glutaraldehyde (diluted from 25%, EM grade, Fluka) with 4% paraformaldehyde (Fluka) in 0.1 M PIPES, pH 7.4 at 293K for 15 minutes. The samples were rinsed three times for 5 minutes each in 0.1 M PIPES, pH 7.4, before postfixation in 0.5% osmium tetroxide (Fluka) in PIPES, pH 6.8 at 293K for 60 minutes. The samples were then rinsed three times for 5 minutes each in double distilled water and stained with 5% aqueous uranyl acetate (Fluka) for 60 minutes at 293K.

Dehydration and embedding

Each fixed sample was taken through an ethanol series: 50%, 70%, 96%, 100% for 15 minutes each, respectively. This was followed by LR White resin (Agar, Stanstead, England) (apart from *Parochis*), for 1-3 hours to allow complete infiltration of the resin into the sample. The *Parochis* parasites were originally prepared for TEM studies in the 1970's having been taken from 100% ethanol before going through 3:1, 1:1, 1:3 ethanol:propylene oxide for 15 minutes each and then into 100% propylene oxide. The propylene oxide was replaced with Araldite resin (Agar) through a 1:1 then 1:3 mixture of propylene oxide:resin for 15 minutes each before infiltration with resin for 1-3 hours. All impregnated samples were placed in gelatin or polyethylene BEEM capsules (Agar), containing fresh resin for polymerization at 338K for 12-16 hours to produce blocks for trimming.

Transfer and coating

The polymerized resin blocks containing the biological samples were removed from the capsules. The blocks were trimmed, centering the specimens in a trapezoidal shaped face of up to 5 mm^2 and ensuring that the block had a smooth finish by shaving it with a glass knife in an ultramicrotome. The resin block sides were then painted with silver paint, leaving only the face and about 2-5 mm below it uncovered. They were placed in a special multi-holder (Fig. 1) and sputter coated with 6-8 nm Ag, Cr or Al (as measured with a quartz thin film monitor, positioned at a fixed place relative to the specimen) in a Baltec MED 020 unit (Baltec, Balzers, Liechtenstein). The trapezoidal face was covered at a slow coating rate of 0.1 nm per second, using a water cooled target. The sputter coater was first run without samples to remove oxide from the target.

Microscope operating conditions

Individual resin blocks were placed in another special holder which was mounted on a "swallow" holder (Fig. 1) on the specimen stage. BSE images of the specimens were acquired using a Hitachi S-4100 field emission SEM (Rahn AG, Zürich, Switzerland) fitted with an Autrata yttrium aluminum garnet (YAG) BSE detector (Institute Scientific Instrumentation, Prague, Czech Republic).

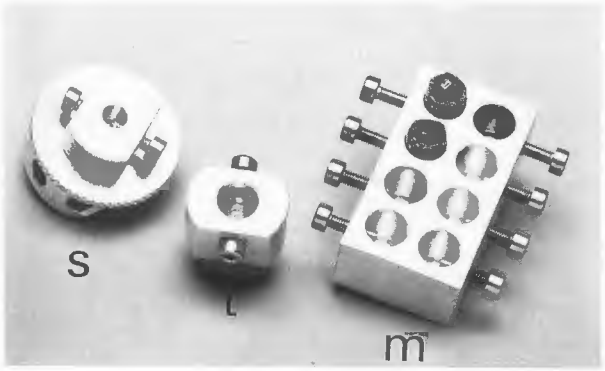

Figure 1. Special holders to allow preparation and use of TEM blocks in the FESEM. An Hitachi "swallow" holder (s) is shown with special mount for TEM stubs attached, a mount for TEM stubs (t) and a multi-holder (m) with two trimmed blocks held within to allow sputter coating.

The microscope was operated at an accelerating voltage of 10 keV and 50 μA emission current. A working distance of 10 mm was used to optimize both resolution and BSE collection. The condenser lens current was maximized (C18), thus minimizing the spot size and the widest objective aperture of 100 mm diameter (number 1) was used to allow more electrons to interact with the specimen. Both normal and inverted signal polarity were used to obtain images comparable both to SEM viewing (heavy metals appearing bright) and TEM viewing (heavy metals appearing dark).

Transmission electron microscopy

Ultrathin sections (60-90 nm) of samples already examined in the SEM were cut on an LKB Ultramicrotome III (Agar). The sections were floated onto Formvar coated copper grids and stained for 5 min. each with 5% uranyl acetate (Watson, 1958) and 5% lead citrate (Reynolds, 1963). Micrographs were taken with a JEOL 100CX (JEOL USA, Peabody, MA) TEM operated at an accelerating voltage of 100 keV.

Results

Secondary electron (SE) imaging provided detail of the surface topography of the resin block and showed clearly where uncoated cracks lay, but gave no information about the embedded specimen (Fig. 2a). With the increased emission current used compared to normal use of the microscope (50 μA instead of 10 μA) the yield of both SE and BSE were increased, so that even "SE" detection with an Everhart-Thornley detector gave a large amount of BSE information (Fig. 2b). BSE imaging gave compositional information from the surface to

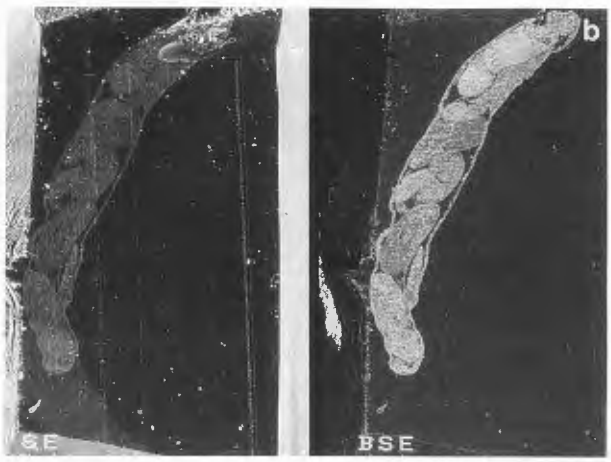

Figure 2a. SE image (at 20 kV) of the surface of a TEM block with surface charging from within uncoated cracks. No detail of the osteoblast cell layer within can be seen. Photo width (P.W.) = 109 μm.

Figure 2b. SE (left) and BSE (right) images (at 10 kV) of cercaria of *Parochis* parasite embedded in Araldite. The SE image (visible due to a larger number of BSE produced at the high emission current used, which forms a small component in the signal detected) is detected with the Everhart-Thornley detector; the BSE image is detected with the YAG detector. P.W. = 1.6 mm.

---

varying depths within the specimen. Specimen damage did not appear to be increased significantly by the increased probe brightness.

The images were two dimensional providing averaged information on the internal structure of the specimen in relation to the depth from which the BSE would be expected to be emitted from. Stereo pair micrographs were taken at -6° and +6°, but no three dimensional information was obtained due to the nature of the detector above the specimen (not shown).

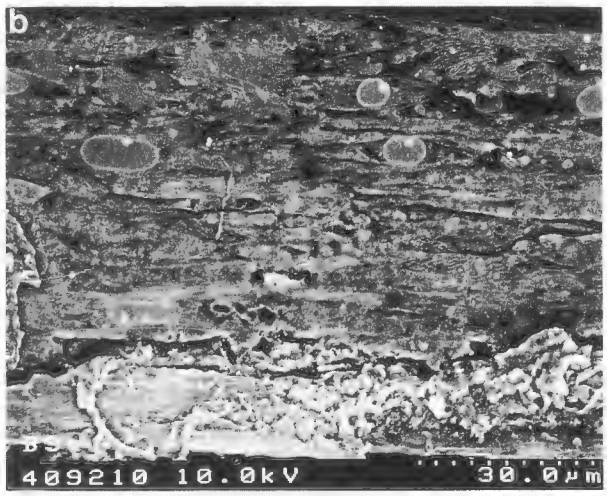

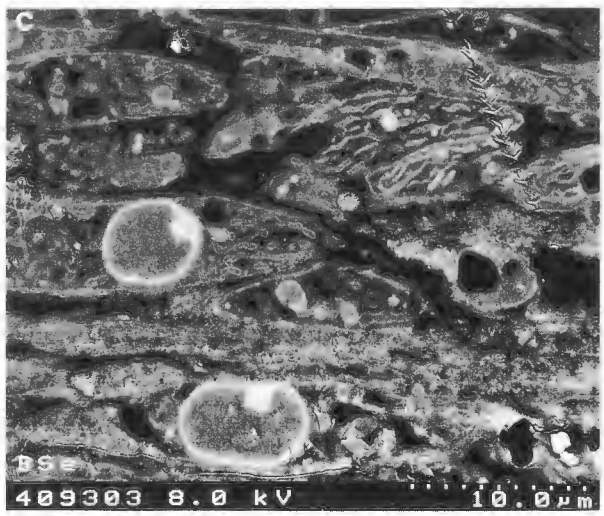

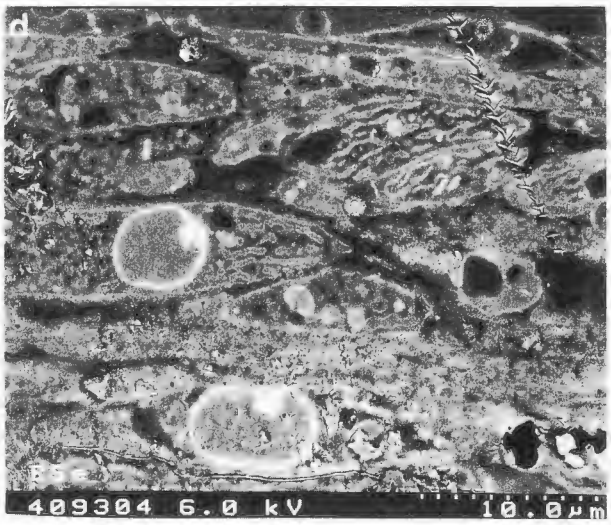

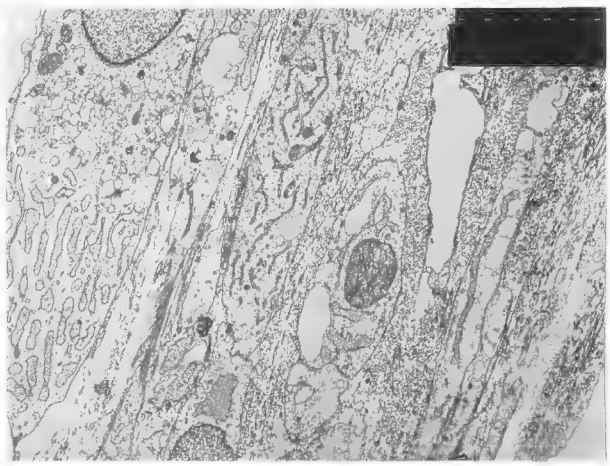

Figure 3. (a) BSE image of the stained osteoblast cell layer within the resin block (as in Fig. 2a). The dedicated BSE detector allows the display of the high contrast image produced at the high emission current. (b) BSE image of the osteoblast layer (as in Figs. 2a and 3a). At this accelerating voltage, there is good contrast of the specimen without hindrance of BSE emitted from greater depths, diffusing image quality. (c) BSE image of the osteoblast layer showing the osmium stained cellular ultrastructure in a transmission electron microscopic style image. The cell membrane, nuclear membrane, nucleolus and endoplasmic reticulum are all evident. (d) BSE image of the osteoblast layer (as in Fig. 3c). The lower accelerating voltage displays a more topographical view of the resin surface with a lower contrast of the specimen within. (e) A transmission electron micrograph (100 keV) of the osteoblast layer (same block as Figs. 2a and 3a-d) after trimming, ultrathin sectioning and post section staining.

P.W. = 104 µm (a and b) and 35 µm (c, d, and e).

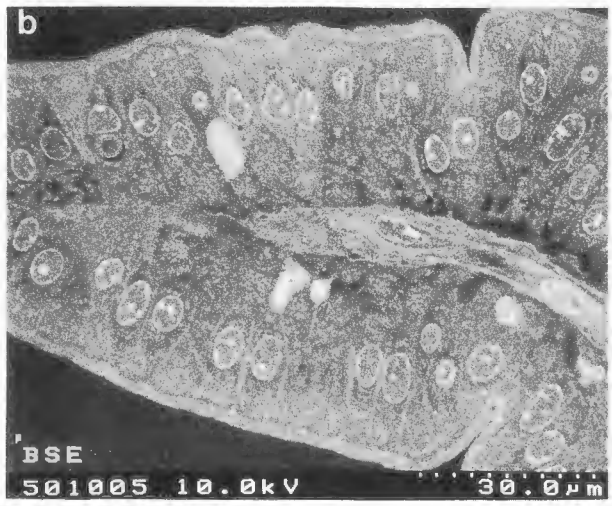

Figure 4. BSE images of transversely sectioned mouse intestine. **(a)** No information of the microvilli is hidden by grid bars which would occur with TEM. P.W. = 730 μm. **(b)** The surrounding brush border of the microvillus, internal cells, nuclear membranes and nucleoli are observed. P.W. = 104 μm.

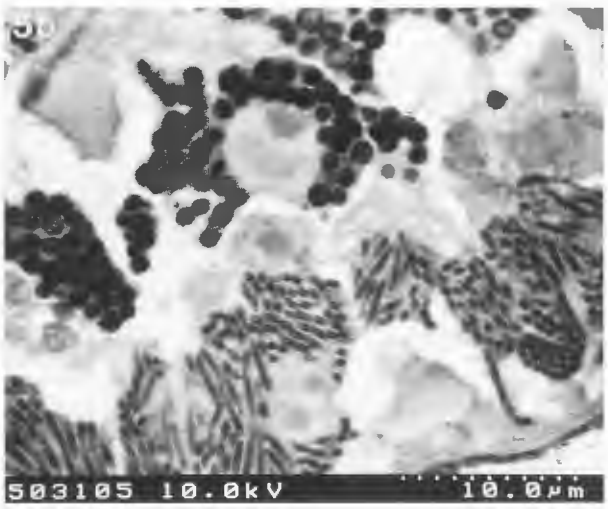

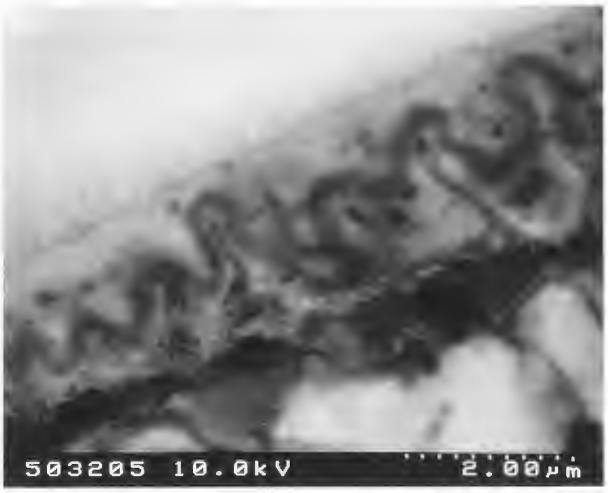

Figure 5. BSE images of cercaria of *Parochis* parasites. **(a)** Highly osmiophilic unsaturated lipid vesicles and other internal organs are made visible by their different osmiophilic levels. P.W. = 73 μm. **(b)** Inverted polarity image where the osmiophilic vesicles appear black. The three dimensional (3D) nature of the elements near the edge of the parasite are seen which could not be observed in TEM without serial sectioning. P.W. = 35 μm. **(c)** Inverted contrast image of the tegument. A greater depth into the specimen is visualized compared to an ultrathin section for TEM; consequently, the 3D arrangement of peripheral villi is seen. There is a very low chance of capturing a whole intact villi attached to the parasite in an ultrathin section. P.W. = 7.3 μm.

Having the lowest density of the metals used for coating, aluminum gave the best image contrast for specimens in the resin blocks. It was also the most difficult metal to coat with since small fluctuations in vacuum pressure (optimally, 6 x 10^{-3} bar for the Baltec MED 020 unit) or coating current (optimally 130 mA) would cause the target to etch the specimen rather than coat it. Before coating the unit had to be operated without specimens in order to remove the oxides from the targets. Specimen storage with aluminum coated samples also presented difficulties due to the high oxidation rate of the coating. On re-examination of a sample a few months after coating the contrast of the specimen within the resin was reduced.

Accelerating voltages greater than 10 keV gave too much electron scattering and penetration within the specimen (Fig. 3a) and also some specimen damage was evident. Accelerating voltages between 8-10 keV were found to give the best results (Figs. 3b and 3c) with good resolution and contrast of the internal structures and a low signal-to-noise ratio.

At lower acceleration voltages than 10 keV, image contrast was reduced and non-useful topographical information from the surface of the block became evident in the image (Fig. 3d). A TEM image taken at an accelerating voltage of 100 keV of an ultrathin section (between 60-90 nm) from the resin block containing the cultured osteoblasts (Figs. 2a and 3a-d) is shown (Fig. 3e). It was seen to give similar results to the BSE image from the FESEM, but without the possibility of viewing at the very low magnification which is possible with the FESEM (Fig. 3a).

Preselection of areas of interest can be made on large block faces (Figs. 4a and 4b) allowing low magnification imaging of cells without the necessity for sectioning. The contrast differences of osmiophilic structures gives good staining of specimens (Fig. 5a) for both the FESEM and, if required, TEM. This removes the necessity for staining of sections required for low power observation using a light microscope (LM).

Inversion of the polarity of images taken with the FESEM (Fig. 5b) allows for a more classical interpretation of the "TEM" style image. The three dimensional structure of specimens which are several hundreds of nanometers deep, such as the ultra-fine villi on the tegument of *Parochis* (Fig. 5c), would be difficult to interpret when studying a series of ultrathin TEM sections. Our method allows easier visualization of the three dimensional aspects of such specimens.

A small imprint of the raster, resulting from the effect of the intense beam under the applied operating conditions, was produced on the block surface during examination in the FESEM, although no damage could be seen to the specimen. This slight damage was not observed during BSE examination, but could be seen with a low power light microscope as a change in light reflection off the face of the block. This was used to identify areas of interest for final trimming for ultrathin sectioning for TEM studies. At higher magnifications than those displayed in the present work, damage to the resin and the specimen was evident during examination. Both Araldite and LR White resin were suitable for this method, and it is probable that other resins could also be used with this technique.

Discussion

At normal operating emission currents up to 20 μA it was shown that {without tilting the specimen block towards the Everhart Thornley (E-T) detector to increase the number of BSE entering it} secondary electron detection only gave topographical information.

The stained specimen within the resin block is detectable with secondary electron detection due to a small percentage of the signal collected being composed of BSE (Everhart *et al* , 1959). Some of the information detected with the secondary electron detector may also be from specimen originated SE-II which are generated by the BSE (Drescher *et al.*, 1970). Since the SE-II signal is a result of backscattering its characteristics support those of the BSE_{II} signal. Both signals can be collected through a E-T detector. The BSE_{II} come from the depth of the specimen and undergo multiple accumulative elastic interactions, spatially disconnecting them from the primary beam. Eventually, they emerge from the surface at a distance from the point of impact. The other class of BSE, BSE_{I} are produced from high elastic-scattering angles causing immediate emergence in the vicinity of the beam impact area and are sensitive to the surface structure. Therefore tilting of the specimen towards the E-T detector and increasing the emission current enhances the level of BSE_{II} and SE-II entering the detector giving the image of the specimen. Obviously, a sophisticated detector such as the Autrata YAG BSE detector will give better results. The Autrata YAG BSE detector was positioned directly under the final lens of the FESEM. It allows the primary beam to pass through a hole in the crystal and high deflection BSE is detected that have been deflected through 180°. This gives atomic number contrast, therefore eliminating nearly all topographical contrast from the specimen which would be generated from low deflected BSE.

The fixation protocol was designed to increase the amount of heavy metals (Os, Z = 76; U, Z = 92), staining the cells in order to provide contrast for BSE detection. Silver (Z = 47), aluminum (Z = 13) and chromium (Z = 24) were chosen to coat the samples, as they have a low density compared to the more common-

ly used gold (Z = 79). Carbon coating of these flat samples could also have been used, but was not available in the laboratory. It is possible that better contrast would be produced with carbon. Low density coating should reduce the number of BSE produced by the coating since the number of BSE produced increases with the atomic number of the sample irradiated. Absorption of BSE by the lower density coating should also be less. The surrounding resin (low Z) does not absorb a significant number of the BSE. The low sputtering rate was used (0.1 nm/s) to give a small particle size and increase the resolution attainable (Echlin *et al.*, 1980).

The approximate depth of an "average" electron penetration into a biological specimen embedded in LR White acrylic resin at an accelerating voltage of 10 keV, estimated using the expression published by Kanaya and Okayama (1972), is about 3 mm. The approximate depth from which BSE would be expected to be emitted from within this embedded specimen would therefore be about 0.8 mm. Semi-thin sections, if required, could therefore also be imaged using this technique. The section thickness would need to be greater than the estimated depth from which BSE would emerge, at the accelerating voltage being used, in order to prevent BSE produced from the holder upon which the sections are mounted from being incorporated into the image. The benefits of the high emission current - BSE detection method are as follows:

1. Low power micrographs of large areas of samples can be made without obscuring of the specimen by grid bars (Figs. 2b, 3b and 4a) as occurs in a TEM and without the requirement for performing extra staining methods on a section of the material for the LM.

2. In all the figures shown, there was no requirement to cut sections. In pathology, a section is usually cut, stained for the LM and then viewed with the LM to select an area of interest before ultrathin sectioning for the TEM. The material required for ultrastructural study can often be in the thick section used for the LM, and therefore, normally eliminated from possible ultrastructural study. There is no requirement for any of these extra steps using this technique. The FESEM can be used for the diagnosis of pathological samples and if subsequent very high magnifications are required, the exact same material can be sectioned for TEM analysis.

3. The heavy metal staining of structures provides good contrast, and therefore, no post-section staining is necessary with this technique and there is no possibility of metal precipitates obscuring regions of interest. Again, if very high magnifications are found to be required, subsequent sectioning and staining for the TEM would have to be performed.

4. The image obtained utilizing the detected BSE emerging from within the calculated approximate depth of specimen (see the Kanaya-Okayama equation) gives three-dimensional (3D) information about the specimen. As the material is not sectioned and at 10 keV BSE is detectable from about the top 0.8 mm of the specimen, material can be observed which would not be present intact within an ultrathin TEM section.

5. The technique allows for the display of the 3D nature of structures within a specimen which could not be observed in an ultrathin section. Serial sectioning would have to be performed to provide the 3D information from conventional TEM sections.

Conclusions

We have demonstrated that an FESEM, fitted with a BSE detector can be used routinely to study fixed, embedded biological samples with good contrast and resolution. The FESEM images generated as a result of optimizing lens current and aperture size settings for the increased number of BSE produced from the high emission current provided useful structural information from the samples studied. It is thought that the technique could be applied to interpretation of some pathological samples without the extra work involved with the application of other stains for LM followed by laborious ultrathin sectioning for TEM. Development of improved fixation and staining procedure for samples specifically for this technique would possibly give even better results. The method also allowed for routine preselection of regions of interest within a biological sample before final trimming and sectioning for TEM study.

Acknowledgements

We thank Philip Lloyd for technical assistance with the TEM and Professor Gwendolen Rees FRS (deceased) for fixed, stained and embedded *Parochis* (University of Wales, Aberystwyth). We also thank Isabelle Gerber for providing the fixed, stained and embedded osteoblasts (AO/ASIF Research Institute, Davos).

References

Drescher H, Reimer L, Seidel H (1970) Backscatter coefficient and secondary electron yield of 10-100 keV electrons and relation to scanning electron microscopy. Z angew Phys **29**: 331-336.

Echlin P, Broers AN, Gee W (1980) Improved resolution of sputter coated films. Scanning Electron Microsc **1980**; I: 163-170.

Everhart TE, Wells OC, Oatley CW (1959) Factors affecting contrast and resolution in the scanning electron microscope. J Electron Control **7**: 97-111.

Goldstein JI, Newbury DE, Echlin P, Joy DC, Romig AD, Lyman CE, Fiori C, Lifshin E (1992) Scanning Electron Microscopy and X-ray Microanalysis. 2nd Edition. Plenum Press, New York. pp. 69-146.

Kanaya K, Okayama S (1972) Penetration and energy-loss theory of electrons in solid targets. J Phys D: Appl Phys **5**: 43-58.

Kushida H, Kushida T, Nagato Y, Ogura K (1982) An improved method for both light and scanning electron microscopy in backscattered electron mode of identical sites in semi-thin sections embedded in GMA and Quetol 523. J Electron Microsc **31**: 202-205.

Nanci A, Zalzal S, Smith CE (1990) Routine use of backscattered electron imaging to visualize cytochemical and autoradiographic reactions in semi-thin plastic sections. J Histochem Cytochem **38**: 403-414.

Reynolds EA (1963) The use of lead citrate at high pH as an electron-opaque stain in electron microscopy. Cell Biol **17**: 208-212.

Richards RG, ap Gwynn I (1995) Backscattered electron imaging of the undersurface of resin-embedded cells by field emission scanning electron microscopy. J Microsc **177**: 43-52.

Scala C, Pasquinelli G, Martegani F, Laschi R (1985) Use of secondary electron detectors for compositional studies on embedded biological material Scanning Electron Microsc **1985**; IV: 1709-1718.

Scala C, Cenacchi G, Apkarian RP, Preda P, Pasquinelli G (1990) Correlative light microscopy, scanning electron microscopy, and transmission electron microscopy of osmium macerated biological tissues. J Electron Microsc **39**: 508-510.

Scala C, Cenacchi G, Preda P, Vici M, Apkarian RP, Pasquinelli G (1991) Conventional and high resolution scanning electron microscopy of biological sectioned material. Scanning Microsc **5**: 135-145.

Watson ML (1958) Staining of tissue section for electron microscopy with heavy metals. J Biophys Biochem Cytol **4**: 475-478.

Wing-Ling NG, Ma L, So KF (1982) Preparation of Epon-embedded renal tissue for scanning electron microscopy. J Clin Pathol **35**: 1384-1387.

Discussion with Reviewers

G.M. Roomans: According to the original paper of Kanaya and Okayama (1972) equation (1) is valid for accelerating voltages over 10 keV, yet you use it for an accelerating voltage of 3 and 6 keV. Please comment.
Authors: We should have stated that for accelerating voltages below 10 keV the equation provides a rough approximation of electron penetration. Though in the images which produced optimal resolution and contrast, an accelerating voltage of 10 keV was used and the equation can be applied.

S.K. Chapman: For those who do not have a dedicated BSE detector, have you tried using the conventional Everhart-Thornley detector, in its SE mode, tilting the specimen to enhance the level of BSE entering the detector? If so, did you need to use a higher accelerating voltage and was the level of BSE data very informative?
Authors: The micrographs shown in Figure 3, which were collected using the standard E-T detector, although mostly displaying SE (I & II) information clearly contain a BSE component. As the specimen was not tilted towards the E-T detector, and SE signal not excluded (by turning off the voltage on the detector grid), then the conditions for collection of BSE were not optimized. No doubt some useful information could be gathered in this way, but we cannot expect this technique to work well with a tilted specimen and an E-T detector which will be at some distance from the specimen. Increasing the accelerating voltage gives the same problems as increasing it in BSE detection mode, giving a more diffuse image due to the greater penetration of the primary beam.

S.K. Chapman: Was there any particular reason why you did not try carbon coating the specimens? They are flat and should coat fairly successfully.
A. Nanci: Have the authors used carbon to coat the specimens and, if so what are its advantages and disadvantages?
Authors: At present, we do not have a carbon coater at this institute. It is probable that, with carbon coating, the contrast of the specimens would be greater.

S.K. Chapman: Have you any experience with less sophisticated BSE detectors, silicon based or scintillator style?
Authors: Not on the FESEM. However, performing the same procedure on a thermionic gun microscope (JEOL 840), using the JEOL solid state BSE detector gave similar, but inferior quality, results. It is not possible to get the same kind of relatively high resolution pictures because of the limitations imposed by the thermionic gun emissions. The detector itself worked quite well and was configured to differentiate by atomic number contrast.

G. Pasquinelli and C. Scala: Did you find any FESEM contamination, e.g., column, diaphragms during sample examination at the used emission current settings? Was your FESEM fitted with a cold trap?
Authors: No contamination has been found as of yet. The microscope is now 2 years old and has had 980 hours of use, with up to one quarter of that time under

high emission currents. The tip noise is minimal and the beam is even stable at 5 μA. It is thought that the high currents even help to keep the tip clean. There is a cold trap which minimizes the possibility of contamination

A. Nanci: Is the method described limited to highly-contrasted tissues? If so, could contrasting treatments limit the choice of resins for embedding and/or the subsequent use of the tissues for further postembedding LM or TEM analysis?
Authors: The method is not limited to highly contrasted specimens, however the inclusion of high atomic number stains in the specimen does, as would be expected, increase the image contrast significantly. We have used the method to view LM sections of unstained bone fixed only in ethanol around implants giving good contrast between the implant/bone/resin interface.

A. Nanci: Since the surface of the bloc must be prepared, there may be little gain in time compared to preparing thick sections for BSE analysis. In this regard and considering the advantages of tissue sections for cytochemical analyses, would the section approach be more flexible?
Authors: Whereas most specimens would need to have the surface of the block prepared by "shaving" with a glass or diamond knife, some specimens, where the material lies close to the resin surface, have been viewed without preparation. Very large areas can also be studied, and there is no risk of loosing sections/section folding, etc. One of the advantages of this approach is that the material which might be taken for later ultrathin sectioning is still in the block and has not had to have been sacrificed to give a light microscope section. There are, clearly, some circumstances where cytochemical staining of sectioned material may be necessary, however, where location of anatomical structures is needed the described method has some advantages. Its use does not exclude the possibility of taking sections subsequently for cytochemical analysis, if it is so desired.

A. Nanci: Can the analysis of the bloc surface, under the conditions used, affect the cutting and/or cytochemical properties of the subsurface tissue?
Authors: The analysis of the bloc sample does not affect the cutting with the microtome. A TEM micrograph of one of the blocks already viewed in the FESEM is presented (Fig. 3e). With all samples viewed by this method, the ensuing ultrathin sectioning and TEM analysis was normal. As far as the possible effects of irradiation upon any subsequent cytochemical investigation of the tissue is concerned, this has not been tested. If accelerating voltages up to about 6 keV have been used, then the likely penetration of electrons into the block is probably less than 1 μm. We cannot tell how deep any thermal effects may penetrate.

A. Nanci: Staining artifacts are not a routine problem in EM analysis, hence elimination or section staining does not appear to be a strong argument in favor of the method described by the authors. Indeed, "en bloc" staining may just as likely result in precipitates. Could the authors elaborate on this comment?
Authors: Though section staining is not a routine problem, if the step is not required, then there is obviously not even a chance of the problem occuring. We have found no problems with any of our en bloc staining techniques.